Received: August 25, 2022. Revised: October 5, 2022. 618

International Journal of
Intelligent Engineering & Systems

http://www.inass.org/

Error Correction Using Hybrid Coding Algorithm for BER Reduction in MIMO-OFDM

Venu Gopal Tikka[1]* **Radhika Sivashanmugam[2]**

[1]*Department of Electronics, Sathyabama Institute of Science and Technology, Chennai, India.*
[2]*Department of Electrical and Electronics Engineering,*
Sathyabama institute of science and technology, Chennai, India
* Corresponding author's Email: venugopalhod@gmail.com

Abstract: The integration of multiple input multiple output (MIMO) - orthogonal frequency division multiplexing (OFDM) has massively received attention due to its reliability, spatial multiplexing gain and improved spatial diversity gain. However, the MIMO-OFDM is affected because of the errors that occurred during the communication such as inter symbol interference, and inter carrier interference (ICI). In this research, the error correction using hybrid coding algorithm (EC-HCA) is proposed for correcting the errors that occurred during the data transmission. The combination of quasi cyclic low-density parity check (QC-LDPC) and space time block coding (STBC) approaches are used in the hybrid coding which helps to achieve better data broadcasting over the MIMO-OFDM. Here, the interference among the transmitting antennas is avoided by using the STBC. Therefore, the ICI and inter symbol interference (ISI) that occurred in the MIMO-OFDM is minimized by the EC-HCA and it leads to achieving less BER. The performance of the EC-HCA method is analyzed by means of the bit error rate (BER) and peak signal to noise ratio (PSNR). The existing researches such as AED, PC-CC and TC-OPA are used to evaluate the performance of the EC-HCA method. The PSNR of the EC-HCA for 2 × 2 MIMO-OFDM is 10.24 dB which is high when compared to the AED, PC-CC and TC-OPA.

Keywords: Bit error rate, Error correction, Hybrid coding algorithm, Multiple input multiple output, Orthogonal frequency division multiplexing, Peak signal to noise ratio.

1. Introduction

Nowadays, MIMO is considered an auspicious approach because of its effective spectrum usage, higher data rate, and transmission capacity through the multipath fading channel [1]. MIMO is the reliable approach that can handle the increasing wireless data traffic of the future generation of a wireless communication network [2]. Moreover, the connection of multiple transmitters and receivers at both ends of the MIMO system is used to increase the channel capacity [3, 4]. OFDM is the essential approach for the mobile communication network because of its higher spectral efficiency [5, 6]. Generally, the OFDM separates the frequency-selective fading channel into various flat fading subchannels. After dividing the channels into subchannels, the cyclic prefix (CP) is incorporated before each OFDM symbol as the guard interval (GI) that performs an effective elimination of inter-symbol interference (ISI). Since, the OFDM is utilized in the various applications of wireless communication such as broadband internet access, mobile, satellite TV, and more wireless networks. Hence, the MIMO is combined with the OFDM to simultaneously enhance the system capacity and data rate [7 - 9].

The main features of the MIMO-OFDM through the single carrier system are resistance to channel fading, robustness against impulse interference, less nonlinear distortion, large power spectral efficiency, ability to handle very strong echoes, uniform average spectral density, and utilization of small guard intervals [10]. Since the wireless channel generates the inherent noise in the communication system

which affects the data broadcasted over the channel. These added noises either reflective, additive, or power absorbing in nature produced an identical effect over the broadcasting data in the wireless channel. The aforementioned noise categories have one parameter in common that is denoted as BER [11]. The constructive addition of numerous subcarriers leads to an increase in the PAPR of the system. Thus, adverse effects such as BER minimization and inter-modulation interference are caused in the OFDM signal [12 - 14]. Therefore, the forward error correction codes are developed for identifying and correcting the errors that occurred in the channel while transmitting the data without any retransmission of the data [15].

The contributions of this paper are concise as follows:

- The combination of quasi cyclic low density parity check (QC-LDPC) and space time block coding (STBC) approaches are used in the hybrid coding helps to achieve better data broadcasting over the MIMO-OFDM.
- Here, the interference among the transmitting antennas is avoided by using the STBC. Therefore, the ICI and ISI that occurred in the MIMO-OFDM are minimized by the EC-HCA and it leads to achieving less BER.

This research paper is arranged as follows: The existing works about the BER minimization in MIMO-OFDM are provided in section 2. The explanation of the proposed method is provided in section 3. Section 4 provides the outcomes of the proposed method whereas the conclusion is presented in section 5.

2. Related work

Yavasoglu [16] implemented the concatenation of Bose Chaudhuri Hocquenghem (BCH) and convolutional code (CC) for OFDM with a multipath fading channel. The interferences were avoided and orthogonality between subcarriers was maintained by using the cyclic prefix (CP) with BCH-CC. Moreover, the impact of interferences was minimized by using the interleaver and CP. The performance of the BCH-CC-OFDM mainly depends on the coding rate of the CC.

Lee [17] presented an iterative schemes-based analog precoding matrix for the MIMO-OFDM system. Additionally, one suitable precoding matrix with higher power than the hybrid precoding matrix was chosen for obtaining the optimal performance. Here, the iterative algorithm was adopted by the hybrid precoding matrix. The value of mean square error (MSE) among optimal and hybrid precoding matrices for both the sub and full-connected architectures were used to update the analog and digital precoding matrix during the iterative process. Subsequently, the precoder with the high power was identified by performing the analog precoding in each iterative process which was used to improve the performance. However, the higher order of FFT affected the performance of the MIMO-OFDM.

Ghazi-Maghrebi and Akbarian [18] implemented the cyclic delay diversity (CDD) and discontinuous doppler diversity (DDoD) based Alamouti encoding and decoding (AED) for enhancing the capacity and reliability. The developed CDD and DDoD-based AED was analyzed using the second-generation terrestrial video broadcasting system. Moreover, the information about the CDD and DDoD wasn't required in the receiver. However, the BER of the DDoD with Alamouti coding has high BER than the conventional Alamouti coding.

Agarwal, and Mehta [19] examined the probability of combining polar codes (PC) and CC for obtaining the error correction in MIMO-OFDM. Here, the PC-CC was analyzed under various modulation schemes such as binary phase shift keying (BPSK), quadrature amplitude modulation (QAM)-16, QAM-64 and quadrature phase shift keying (QPSK). The interference that occurred during the communication was minimized by using PC-CC. However, this work failed to consider the mapping of rectified bits during the communication.

Pyla [20] presented the optimal power allocation (OPA), coding, and channel estimation for enhancing the capacity and BER. The statistics of SNR using the singular value decomposition and water filling algorithm were used to perform the adaptive distribution of power in OPA. Here, a less amount of channels was chosen for OPA, when the system has less SNR. The comb-type pilot channel estimation was done by using the minimum mean square error, least mean square (LMS) and least square estimators. The coding was done by using the turbo code (TC) with the coding rate of $1/2$ and $1/3$ which was used to minimize the errors. However, the step size increment in LMS affected the performance of MIMO-OFDM.

3. EC-HCA method

In this research, the EC-HCA method is developed for correcting the errors that occurred during the data transmission. The combination of QC-LDPC and STBC approaches are used in the hybrid coding helps to achieve better data

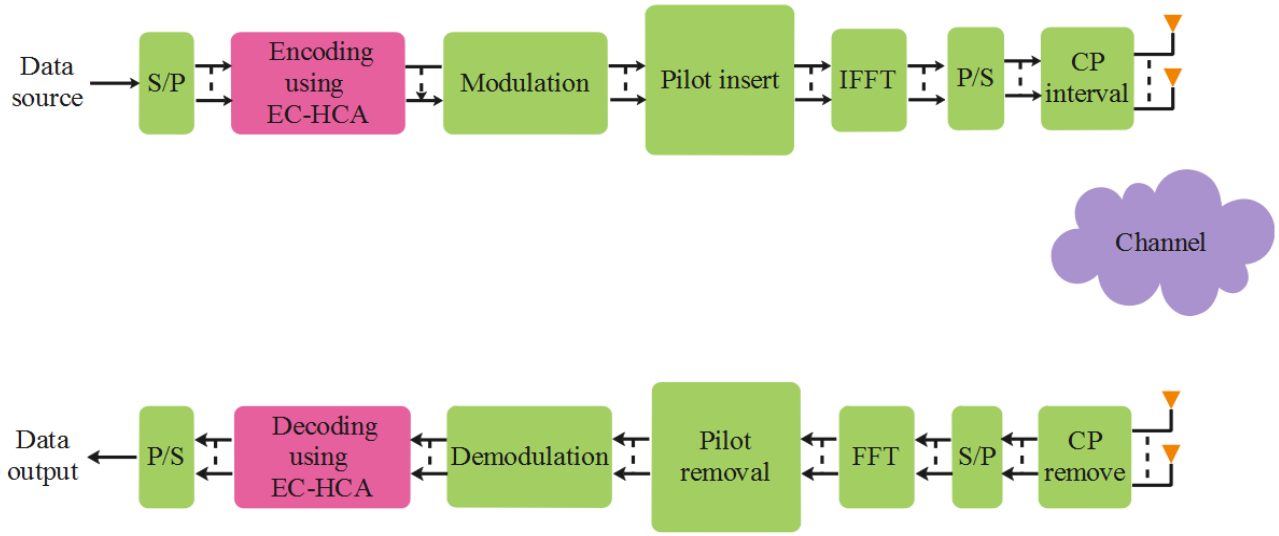

Figure 1. Block diagram of the EC-HCA with MIMO-OFDM

broadcasting over the MIMO-OFDM. Here, the interference among the transmitting antennas are avoided using the STBC. Therefore, the ICI and ISI that occurred in the MIMO-OFDM are minimized by the EC-HCA and it leads to achieving less BER. Fig. 1 shows the block diagram of the EC-HCA with MIMO-OFDM.

3.1 MIMO-OFDM system model

The system model of MIMO-OFDM generally has three portions such as a transmitter, a channel, and a receiver. Consider the MIMO-OFDM system has N_t amount of transmitting antennas and N_r amount of receiving antennas and N_c amount of OFDM subcarriers. Each data frame is encoded using the EC-HCA method followed by the QAM modulation which is performed over the encoded bits. Subsequently, the serial data is transformed into parallel data and inverse fast fourier transform (IFFT) is employed for converting the symbols into time-domain samples s_α which is expressed in Eq. (1).

$$s_\alpha(n) = \frac{1}{\sqrt{N}} \sum_{k=0}^{N-1} S_\alpha(k)\, e^{j2\pi kn/N}, 0 \le k \le N-1 \quad (1)$$

Where the transmitting antenna's index is represented as α, consider $\alpha = 1,2$; FFT's length is expressed as N which is equal to 256; the index of subcarriers is expressed as k and OFDM symbol is denoted as n.

The guard interval is incorporated for minimizing the inter-symbol and inter-carrier interferences. After multiplexing, the symbols are transformed into a serial stream followed by the signal broadcasting which is accomplished through the AWGN channel. Subsequently, the signal is traversed in the wireless channel and is collected by the receiver. The signal gathered by the MIMO-OFDM receiver (Y_β) is expressed in Eq. (2).

$$Y_\beta(k) = \sum_\alpha^2 H_{\alpha,\beta}(k) S_\alpha(k) + W(k) \quad (2)$$

Where the receiving antenna's index is represented as β, consider $\beta = 1,2$, and noise that occurred through the wireless channel is $W(k)$.

On the receiver side, the cyclic prefix is neglected and symbols are again converted into the frequency domain using the fast fourier transform (FFT) as shown in Eq. (3).

$$Y_\beta(k) = \frac{1}{\sqrt{N}} \sum_{n=0}^{N-1} y_\beta(n)\,(k) e^{-j2\pi kn/N}, 0 \le n \le N-1 \quad (3)$$

Where, y_β is the discrete time domain signal. After converting the symbols to the frequency domain, QAM demodulation and EC-HCA decoding are performed to get the input signal in the receiver. A detailed explanation of the error correction code is given in the following section.

3.2 Error correction using hybrid coding algorithm (EC-HCA)

The EC-HCA is the combination of QC-LDPC and STBC approaches. Initially, the data is given as input to the EC-HCA where the encoding is done to minimize the errors. In EC-HCA, the data is given to the QC-LDPC followed by the encoded data from QC-LDPC is given as input to the STBC. In general, the LDPC is a linear block code having the ability for

avoiding burst errors. This LDPC is represented by using a very sparse parity check matrix that has mainly 0's and few 1's. The multiplication among the uncoded word u of l bits length and the generator matrix of $(G_{l\times BL})$ is generated the codeword v of bits length BL, hence the code rate is $R = l/BL$. The parity check matrix H_{LDPC} of the size $M \times BL$, where $M = BL - l$ represents the set of parity check expressions that are required to satisfy the authentication of codeword as shown in Eq. (4).

$$H_{LDPC} \times v^T = 0 \ (\mathrm{mod}\Theta) \tag{4}$$

Further, the parity check matrix of QC-LDPC has square sub-matrices $Z \times Z$ through the Galois field that are either zero matrix or identifies matrix's cyclic permutation. Here, the parity check matrix of QC-LDPC is developed from $M_{prot} \times BL_{prot}$ and prototype matrix H_{prot} in that, each entry of H_{prot} is swapped by using $Z \times Z$ cyclic shift matrix P^c is expressed in Eq. (5).

$$P^c = \prod_{i=1}^{c} [P^1]_i \quad for\ c > 0 \tag{5}$$

Where, c is the number of equivalent inputs in the matrix H_{prot} and P^1 is expressed in the following Eq. (6).

$$[P^1]_{i,j} = \begin{cases} 1, & (i \bmod Z) + 1 = j \\ 0, & Otherwise \end{cases} \tag{6}$$

Where j represents the parity bit; $P^0 = I_z$; I denotes the identity matrix and $P^- = 0_{Z\times Z}$.

The following condition (7) is required to be satisfied by the all H_{prot}. The prototype matrix values of the parity check matrix are required to be less than the cyclic shift matrix values for all code word and parity bits.

$$\left[H_{prot}\right]_{i,j} < Z \ (\forall\ i, j) \tag{7}$$

The QC-LDPC's parity check matrix of the size $M = Z \times M_{prot}$ and $BL = Z \times BL_{prot}$. Here, the messages are iteratively transmitted among the linked variable nodes and check nodes during the QC-LPDC decoding process. The ratio of posteriori probability log-likelihood for bit i of a broadcasted codeword c_i expressed in Eq. (8) is given as input to the QC-LPDC.

$$L(c_i) = \log\left(\frac{P(c_i=0\,|Y_i)}{P(c_i=1\,|Y_i)}\right) \tag{8}$$

Where the channel output for c_i is Y_i.

The encoded data from the QC-LDPC is given as input to the STBC for further encoding of data. Each information collected from the antenna is integrated using this STBC which is chosen because of its easy computation and high diversity gain. Consider, m is the encoded data from the QC-LDPC and this data is again encoded using the Alamouti STBC for the data symbols q through the duration D and $D + 1$. Eq. (9) summarizes each data's time instance along the varied duration.

$$\begin{aligned} m_1(D) &= q(D) \\ m_2(D) &= q(D+1) \\ m_1(D+1) &= q^*(D+1) \\ m_2(D+1) &= q^*(D) \end{aligned} \tag{9}$$

Where, the complex conjugate is denoted by using $*$.

Similar to the transmitter, the channel response over the receiver CR_{ij} from jth transmitter and ith receiver is included in the output of STBC Eq. (10).

$$\begin{aligned} r_{1i}(D) &= CR_{il}q(D) + CR_{i2}q(D+1) + W(D) \\ r_{1i}(D) &= -CR_{il}q^*(D+1) + CR_{i2}q^*(D) \\ &\quad + W(D+1) \end{aligned} \tag{10}$$

Where, output from STBC is r; q defines the data symbols and W defines the noise that occurred in the system. Therefore, the development of EC-HCA i.e., QC-LDPC with STBC is used to minimize the errors that occurred during communication. Thus, the BER of the MIMO-OFDM is minimized while transmitting the data by correcting the numerous errors that occurred in the communication.

4. Results and discussion

This section provides the outcomes of the EC-HCA method. The implementation and simulation of EC-HCA with MIMO-OFDM are done using the MATLAB R2018a software. This simulation is accomplished with the system configuration of an i5 processor and 6GB RAM. The EC-HCA is analyzed with different antenna configurations such as $2 \times 2, 2 \times 4$, and 4×4. The modulation and channel model used for this EC-HCA method is 16 QAM and AWGN channel whereas the simulation parameters are mentioned in Table 1.

The performance of the proposed EC-HCA

Table 1. Simulation parameters

Parameter	Value
Antenna configurations	$2 \times 2, 2 \times 4$ and 4×4
Modulation type	16 QAM
Number of frames	10,000

Table 2. Comparative analysis of BER for EC-HCA with 2×2 MIMO-OFDM

SNR (dB)	AED [18]	PC-CC [19]	TC-OPA [20]	EC-HCA
1	5.0238×10^{-2}	2.5119×10^{-1}	2.5119×10^{-2}	1.0048×10^{-2}
2	2.0000×10^{-2}	1.0000×10^{-1}	1.0000×10^{-2}	4.0000×10^{-3}
3	7.9621×10^{-3}	3.9811×10^{-2}	3.9811×10^{-3}	1.5924×10^{-3}
4	3.1698×10^{-3}	1.5849×10^{-2}	1.5849×10^{-3}	6.3396×10^{-4}
5	1.2619×10^{-3}	6.3096×10^{-3}	6.3096×10^{-4}	2.5238×10^{-4}
6	5.0238×10^{-4}	2.5119×10^{-3}	2.5119×10^{-4}	1.0048×10^{-4}
7	2.0000×10^{-4}	1.0000×10^{-3}	1.0000×10^{-4}	4.0000×10^{-5}
8	6.3246×10^{-5}	3.1623×10^{-4}	3.1623×10^{-5}	1.2649×10^{-5}
9	2.0000×10^{-5}	1.0000×10^{-4}	1.0000×10^{-5}	4.0000×10^{-6}
10	6.3246×10^{-6}	3.1623×10^{-5}	3.1623×10^{-6}	1.2649×10^{-6}

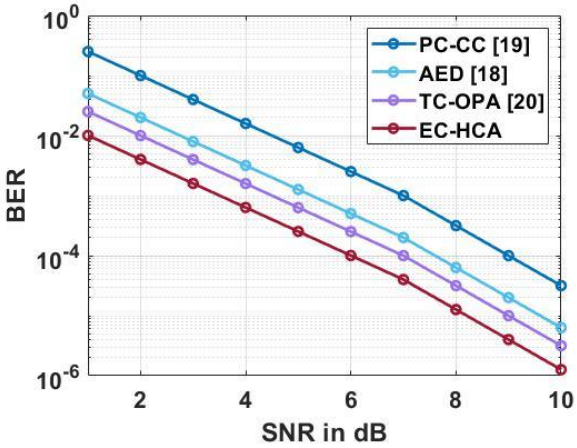

Figure. 2 BER of EC-HCA for 2 × 2 MIMO-OFDM

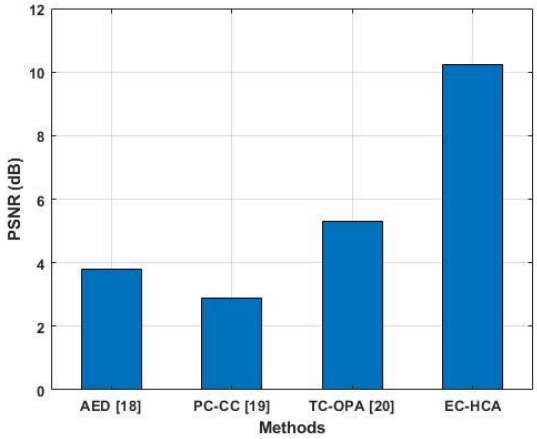

Figure. 3 PSNR of EC-HCA for 2 × 2 MIMO-OFDM

method is analyzed with three different existing types of research namely AED [18], PC-CC [19] and TC-OPA [20]. The EC-HCA method is analyzed in terms of BER and PSNR.

4.1 Performance analysis of EC-HCA for 2×2 antenna

The BER and PSNR of the EC-HCA method for 2 × 2 antenna configuration are analyzed in this section. In this analysis, both the transmitter and receiver are initialized with the 2 antennas. Fig. 2 and Table 2 show the BER of EC-HCA with AED [18], PC-CC [19] and TC-OPA [20] for a 2 × 2 antenna. From the figures and tables, it is known that the EC-HCA has lesser BER when compared to the AED [18], PC-CC [19] and TC-OPA [20]. The hybrid QC-LDPC and STBC of EC-HCA are used to minimize the errors that occurred while transmitting the data frames. Specifically, the space orthogonal pattern minimizes the errors that occurred between the transmitting antennas. Thus, the BER of the EC-HCA method is lesser than the AED [18], PC-CC [19] and TC-OPA [20].

Table 3. Comparative analysis of PSNR for EC-HCA with 2 × 2 MIMO-OFDM

Methods	PSNR (dB)
AED [18]	3.8
PC-CC [19]	2.9
TC-OPA [20]	5.3
EC-HCA	10.24

Moreover, the PSNR of EC-HCA with AED [18], PC-CC [19] and TC-OPA [20] for the 2 × 2 antenna is shown in Fig. 3 and Table 3. Accordingly, the minimization of error increases the PSNR of the EC-HCA method more than the AED [18], PC-CC [19] and TC-OPA [20].

4.2 Performance analysis of EC-HCA for 2×4 antenna

This section shows the analysis of the EC-HCA method with 2 × 4 antenna configuration. Here, the transmitter is fixed with antennas, and the received is fixed with 4 antennas. The BER of the 2 × 4 antenna for EC-HCA with AED [18], PC-CC [19] and TC-OPA [20] is shown in Fig. 4 and Table 4. From the analysis, it is known that the BER of EC-HCA is less when compared to the AED [18], PC-CC [19] and TC-OPA [20]. The combination of QC-LDPC and STBC in the EC-HCA creates a reliable data transmission which results in less errors. The errors of ISI and ICI are minimized by using developed

Table 4. Comparative analysis of BER for EC-HCA with 2×4 MIMO-OFDM

SNR (dB)	AED [18]	PC-CC [19]	TC-OPA [20]	EC-HCA
1	2.3148×10^{-2}	1.0000×10^{-1}	8.1169×10^{-3}	4.9092×10^{-3}
2	5.8146×10^{-3}	2.5119×10^{-2}	2.0389×10^{-3}	1.2331×10^{-3}
3	7.3201×10^{-4}	3.1623×10^{-3}	2.5668×10^{-4}	1.5524×10^{-4}
4	1.8387×10^{-4}	7.9433×10^{-4}	6.4475×10^{-5}	3.8995×10^{-5}
5	3.6687×10^{-5}	1.5849×10^{-4}	1.2864×10^{-5}	7.7805×10^{-6}
6	5.8146×10^{-6}	2.5119×10^{-5}	2.0389×10^{-6}	1.2331×10^{-6}
7	1.1602×10^{-6}	5.0119×10^{-6}	4.0681×10^{-7}	2.4604×10^{-7}
8	1.8387×10^{-7}	7.9433×10^{-7}	6.4475×10^{-8}	3.8995×10^{-8}
9	2.3148×10^{-8}	1.0000×10^{-7}	8.1169×10^{-9}	4.9092×10^{-9}
10	2.3148×10^{-9}	1.0000×10^{-8}	8.1169×10^{-10}	4.9092×10^{-10}

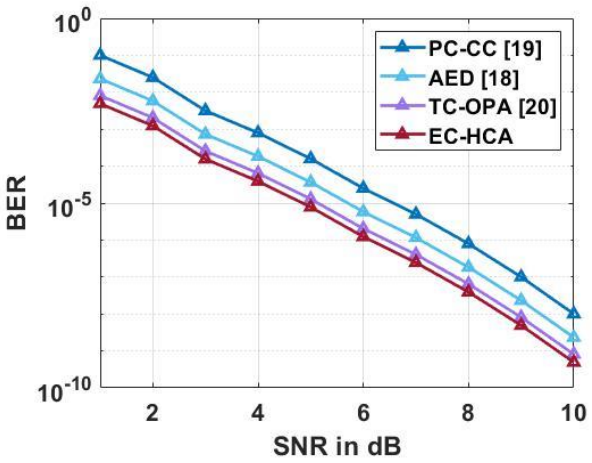

Figure. 4 BER of EC-HCA for 2 × 4 MIMO-OFDM

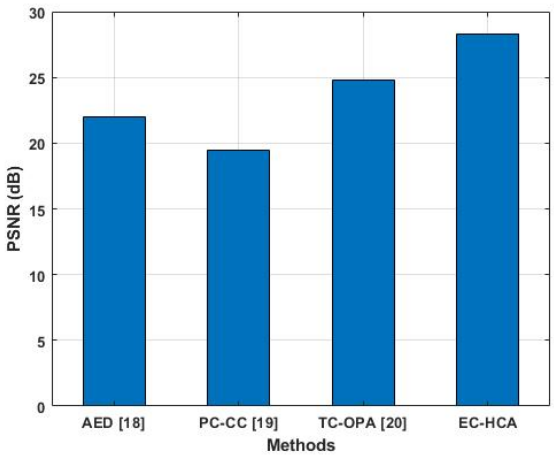

Figure. 5 PSNR of EC-HCA for 2 × 4 MIMO-OFDM

hybrid coding that is used to achieve less BER.

Fig. 5 and Table 5 show the PSNR analysis of EC-HCA method for antenna configuration of 4 × 4. This evaluation shows that the EC-HCA method achieves higher PSNR when compared to the AED [18], PC-CC [19] and TC-OPA [20]. In EC-HCA, the errors that occurred over the MIMO-OFDM are less because of the error correction done by using a hybrid QC-LDPC and STBC algorithm. Accordingly, the

Table 5. Comparative analysis of PSNR for EC-HCA with 2 × 4 MIMO-OFDM

Methods	PSNR (dB)
AED [18]	22.01
PC-CC [19]	19.46
TC-OPA [20]	24.76
EC-HCA	28.33

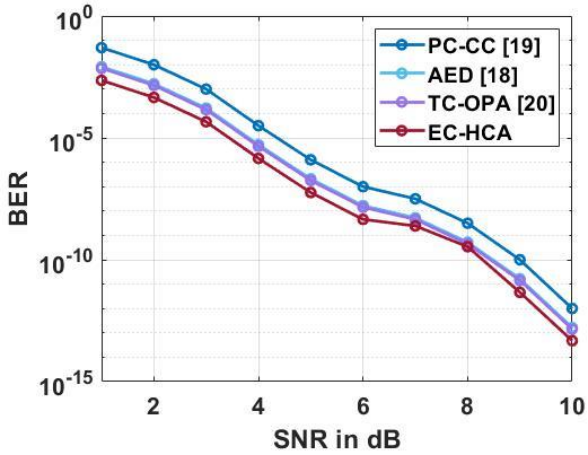

Figure. 6 BER of EC-HCA for 4 × 4 MIMO-OFDM

EC-HCA results in a higher PSNR over the MIMO-OFDM.

4.3 Performance analysis of EC-HCA for 4×4 antenna

The BER and PSNR of the EC-HCA method for 4 × 4 antenna configuration are analyzed in this section. In this analysis, both the transmitter and receiver are initialized with the 4 antennas. Fig. 6 and Table 6 show the BER of EC-HCA with AED [18], PC-CC [19] and TC-OPA [20] for a 4 × 4 antenna. From the figures and tables, it is known that the EC-HCA has lesser BER when compared to the AED [18], PC-CC [19] and TC-OPA [20]. The interference among the antennas is avoided by using the developed EC-HCA, therefore, the ICI and ISI that occurred in the MIMO-OFDM are minimized than the AED [18], PC-CC [19] and TC-OPA [20].

Table 6. Comparative analysis of BER for EC-HCA with 4×4 MIMO-OFDM

SNR (dB)	AED [18]	PC-CC [19]	TC-OPA [20]	EC-HCA
1	8.3116×10^{-3}	5.0119×10^{-2}	7.1293×10^{-3}	2.2792×10^{-3}
2	1.6584×10^{-3}	1.0000×10^{-2}	1.4225×10^{-3}	4.5475×10^{-4}
3	1.6584×10^{-4}	1.0000×10^{-3}	1.4225×10^{-4}	4.5475×10^{-5}
4	5.2442×10^{-6}	3.1623×10^{-5}	4.4983×10^{-6}	1.4381×10^{-6}
5	2.0878×10^{-7}	1.2589×10^{-6}	1.7908×10^{-7}	5.7250×10^{-8}
6	1.6584×10^{-8}	1.0000×10^{-7}	1.4225×10^{-8}	4.5475×10^{-9}
7	5.2442×10^{-9}	3.1623×10^{-8}	4.4983×10^{-9}	2.4381×10^{-9}
8	5.2442×10^{-10}	3.1623×10^{-9}	4.4983×10^{-10}	3.4381×10^{-10}
9	1.6584×10^{-11}	1.0000×10^{-10}	1.4225×10^{-11}	4.5975×10^{-12}
10	1.6584×10^{-13}	1.0000×10^{-12}	1.4225×10^{-13}	4.7775×10^{-14}

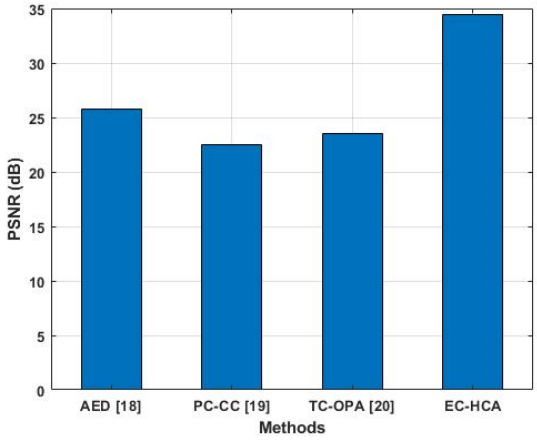

Figure. 7 PSNR of EC-HCA for 4 × 4 MIMO-OFDM

Table 7. Comparative analysis of PSNR for EC-HCA with 4 × 4 MIMO-OFDM

Methods	PSNR (dB)
AED [18]	25.79
PC-CC [19]	22.46
TC-OPA [20]	23.55
EC-HCA	34.48

Moreover, the PSNR of EC-HCA with AED [18], PC-CC [19] and TC-OPA [20] for the 4 × 4 antenna is shown in Fig. 7 and Table 7. Generally, the PSNR of the MIMO-OFDM is inversely proportional to the BER. The less BER of EC-HCA automatically results in higher PSNR than the AED [18], PC-CC [19] and TC-OPA [20].

5. Conclusion

The hybrid coding used for the error correction is the combination of QC-LDPC and STBC approaches. Initially, the data is given as input to the QC-LDPC followed by the encoded data from QC-LDPC which is given as input to the STBC. The guard interval is incorporated for minimizing the inter-symbol and inter-carrier interferences. Therefore, the development of EC-HCA i.e., QC-LDPC with STBC is used to minimize the errors that occurred during communication. Thus, the BER of the MIMO-OFDM is minimized while transmitting the data by correcting the numerous errors that occurred in the communication. From the results, it is concluded that the EC-HCA provides better performance in terms of BER and PSNR than the AED, PC-CC and TC-OPA. The PSNR of the EC-HCA for 2 × 2 MIMO-OFDM is 10.24 dB which is high when compared to the AED, PC-CC and TC-OPA. However, PAPR minimization is also a challenging task, so in the future, an effective PAPR reduction can be developed for improving the performances of MIMO-OFDM.

Conflicts of interest

The authors declare no conflict of interest.

Author contributions

The paper conceptualization, methodology, software, validation, formal analysis, investigation, resources, data curation, writing—original draft preparation, writing—review and editing, visualization, have been done by 1st author. The supervision and project administration, have been done by 2nd author.

Notation list

Parameter	Description
s_α	Time-domain samples
α	Transmitting antenna's index
N	Length of FFT
k	Index of subcarriers
n	OFDM symbol
Y_β	Received signal
β	Receiving antenna's index
$W(k)$	Noise
y_β	Discrete time domain signal
u	Uncoded word
l	Length of uncoded word
$G_{l\times BL}$	Generator matrix
BL	Length of generator matrix
v	Codeword
H_{LDPC}	Parity check matrix

$Z \times Z$	Square sub-matrices
H_{prot}	Prototype matrix
P^c	Cyclic shift matrix
c	Number of equivalent inputs
I	Identity matrix
m	Encoded data from the QC-LDPC
q	Data Symbols
D	Duration
CR_{ij}	Channel response
r	Encoded data from the STBC

References

[1] M. Rakshit, S. Bhattacharjee, J. Sanyal, and A. Chakrabarti, "H0ybrid turbo coding PTS with enhanced switching algorithm employing de to carry out a reduction in PAPR in AUL-based MIMO-OFDM", *Arabian Journal for Science and Engineering*, Vol. 45, No. 3, pp. 1821-1839, 2020.

[2] S. Jothi and A. Chandrasekar, "An Efficient Modified Dragonfly Optimization Based MIMO-OFDM for Enhancing QoS in Wireless Multimedia Communication", *Wireless Personal Communications*, Vol. 122, No. 2, pp. 1043-1065, 2022.

[3] K. Nagarajan and S. Sophia, "Multilevel Redundant Discrete Wavelet Transform (ML-RDWT) and optimal Red Deer algorithm (ORDA) centred approach to mitigate the effect of ICI, BER and CIR in a MIMO-OFDM System", *Wireless Personal Communications*, pp. 1-24, 2021.

[4] J. Karthika, G. Thenmozhi, and M. Rajkumar, "PAPR reduction of MIMO-OFDM system with reduced computational complexity SLM scheme", *Materials Today: Proceedings*, Vol. 37, pp. 2563-2566, 2021.

[5] Q. Wu, X. Zhou, C. Wang, and H. Cao, "Variable pilot assisted channel estimation in MIMO-OFDM system with STBC and different modulation modes", *EURASIP Journal on Wireless Communications and Networking*, Vol. 2022, No. 1, pp. 1-13, 2022.

[6] S. Nandi, N. N. Pathak, and A. Nandi, "A novel adaptive optimized fast blind channel estimation for cyclic prefix assisted space–time block coded MIMO-OFDM systems", *Wireless Personal Communications*, Vol. 115, No. 2, pp. 1317-1333, 2020.

[7] M. Zhang, X. Zhou, and C. Wang, "Time-varying sparse channel estimation based on adaptive average and MSE optimal threshold in STBC MIMO-OFDM systems", *IEEE Access*, Vol. 8, pp. 177874-177895, 2020.

[8] R. Bhandari and S. Jadhav, "Novel spectral efficient technique for MIMO-OFDM channel estimation with reference to PAPR and BER analysis", *Wireless Personal Communications*, Vol. 104, No. 4, pp. 1227-1242, 2019.

[9] C. Venkateswarlu and N. V. Rao, "Optimal channel estimation and interference cancellation in MIMO-OFDM system using MN-based improved AMO model", *The Journal of Supercomputing*, pp. 1-23, 2021.

[10] M. Vijayalakshmi and K. R. Reddy, "An effective hybrid approach for PAPR reduction in MIMO-OFDM", *Analog Integrated Circuits and Signal Processing*, Vol. 102, No. 1, pp. 145-153, 2020

[11] P. Subramanium and R. D. Raut, "AI-enabled turbo-coded OFDM system for improved BER performance", *The Journal of Supercomputing*, Vol. 76, No. 6, pp. 4338-4348, 2020.

[12] A. Singal and D. Kedia, "Performance analysis of MIMO-OFDM system using SLM with additive mapping and U2 phase sequence for PAPR reduction", *Wireless Personal Communications*, Vol. 111, No. 3, pp. 1377-1390, 2020.

[13] R. Chauhan, N. Sood, and I. Saini, "PAPR reduction of MIMO-OFDM using galaxy inspired swarm-based PTS strategy", *International Journal of Systems, Control and Communications*, Vol. 12, No. 1, pp. 72-89, 2021.

[14] K. Nageswaran, M. Selvan, and M. Gandhi, "A Hybrid Transform for Reduction of Peak to Average Power Ratio in OFDM System", *Wireless Personal Communications*, Vol. 118, No. 4, pp. 3187-3197, 2021.

[15] A. Agarwal and S. N. Mehta, "Examining impacts of spatial correlation in forward error correction code", *New Review of Information Networking*, Vol. 25, No. 1, pp. 1-36, 2020.

[16] O. Yavasoglu, N. Akcam, and T. Okan, "Performance analysis of concatenated BCH and convolutional coded OFDM system", *International Journal of Electronics*, Vol. 107, No. 10, pp. 1574-1587, 2020.

[17] S. Lee, W. S. Lee, J. H. Ro, Y. H. You, and H. K. Song, "Hybrid precoding technique with iterative algorithm for MIMO-OFDM system", *IEEE Access*, Vol. 8, pp. 171423-171434, 2020.

[18] S. G. Maghrebi and B. Akbarian, "Improved Performance of Alamouti Scheme Using Cyclic Delay Diversity and Doppler Diversity for MIMO Systems-Based", *Wireless Personal Communications*, Vol. 116, No. 3, pp. 1971-1992, 2021.

[19] A. Agarwal and S. N. Mehta, "PC-CC: An advancement in forward error correction using polar and convolutional codes for MIMO-OFDM system", *Journal of King Saud University-Computer and Information Sciences*, Vol. 32, No. 8, pp. 917-927, 2020.

[20] S. Pyla, "Capacity and BER performance improvement in integrated MIMO-OFDM system using optimal power allocation, channel estimation, and turbo coding", *International Journal of Communication Systems*, Vol. 34, No. 14, p. e4915, 2021.